Published in final edited form as:
Biomaterials. 2010 December ; 31(36): 9373–9381. doi:10.1016/j.biomaterials.2010.07.078.

Biocompatibility of adhesive complex coacervates modeled after the Sandcastle glue of *P. californica* for craniofacial reconstruction

Brent D. Winslow, **Hui Shao**, **Russell J. Stewart**, and **Patrick A. Tresco**
The Keck Center for Tissue Engineering, Department of Bioengineering, College of Engineering, University of Utah, 20 S 2030 E Building, 570 BPRB, Room 108D, Salt Lake City, UT 84112, USA

Abstract

Craniofacial reconstruction would benefit from a degradable adhesive capable of holding bone fragments in three-dimensional alignment and gradually being replaced by new bone without loss of alignment or volume changes. Modeled after a natural adhesive secreted by the sandcastle worm, we studied the biocompatibility of adhesive complex coacervates *in vitro* and *in vivo* with two different rat calvarial models. We found that the adhesive was non-cytotoxic and supported the attachment, spreading, and migration of a commonly used osteoblastic cell line over the course of several days. In animal studies we found that the adhesive was capable of maintaining three-dimensional bone alignment in freely moving rats over a 12 week indwelling period. Histological evidence indicated that the adhesive was gradually resorbed and replaced by new bone that became lamellar across the defect without loss of alignment, changes in volume, or changes in the adjacent uninjured bone. The presence of inflammatory cells was consistent with what has been reported with other craniofacial fixation methods including metal plates, screws, tacks, calcium phosphate cements and cyanoacrylate adhesives. Collectively, the results suggest that the new bioadhesive formulation is degradable, osteoconductive and appears suitable for use in the reconstruction of craniofacial fractures.

Keywords

Bone repair; Osseointegration; Osteoconduction; Biocompatibility; Foreign body response

Introduction

Traumatic injury to the face and skull can create many bone fragments that are difficult to accurately reposition with pins, plates, and screws [1, 2]. In some cases due to the fixation technology in use small bone fragments may be discarded [3-5]. Precise alignment and fixation of severe craniofacial injuries, where cosmetic outcome is a major concern, would benefit from a fixation technology capable of holding bone fragments in alignment while they heal and then disappear to avoid the sequela associated with a persistent foreign body response (FBR). Despite incentives to create such a fixation technology, there are no adhesives in clinical use for craniofacial fracture repair that exhibit these properties.

Developing a bone adhesive is a challenging problem. The adhesive must bond to bone in the wet, bloody, ionically-rich environment of the extracellular space, and neither shrink nor swell significantly during or after curing. The delivery method must be simple. The adhesive must be non-cytotoxic as delivered as well as during subsequent breakdown. The adhesive must allow for the precise repositioning of the fractured bones, as well as maintaining their three-dimensional alignment and fixation during healing. The fixation should be robust to allow the patient free mobility after reconstruction. Inflammation should be commensurate with the healing process and subside as the adhesive is resorbed. The adhesive should not interfere with osteosynthesis at the fracture site or induce changes in the adjacent bone or soft tissues. Finally, the adhesive should eventually disappear to extinguish the FBR and its associated sequela. With regard to the currently available technology, a clinically satisfactory solution requires trade-offs in these specifications; cyanoacrylate adhesives have high fixation strengths but are not degradable and exhibit cytotoxicity, while bioadhesives, like fibrin, are degradable but lack sufficient bond strength [6].

Numerous aquatic organisms, freshwater and marine, produce underwater adhesives highly adapted to specific functions ranging from sessile fixation, to prey capture, to construction of protective shelters. In the latter category, the Sandcastle worm (*Phragmatopoma californica*) assembles fragmented bits of seashells into tubular underwater dwellings with minute dabs of a proteinaceous bioadhesive [7]. The sandcastle glue is adapted precisely for joining biogenic minerals together underwater. From this perspective, it is an excellent model for a biomimetic adhesive for crainiofacial fracture repair.

The natural glue is comprised of a set of oppositely charged proteins complexed with calcium and magnesium ions. The positively charged proteins contain basic residues with amine sidechains; while the negatively charged proteins contain extensive segments of acidic phosphoserine residues [8, 9]. In total, approximately 20 and 30 mol% of the adhesive amino acid residues are basic and acidic, respectively. Analogs of the adhesive proteins were created with a set of oppositely charged synthetic copolyelectrolytes containing the same chemical side chains (phosphates and amines) in the same mol% as the natural proteins. When mixed in water at physiological pH and with roughly equimolar ratios of positive and negative charges the synthetic copolyelectrolytes associated and phase separated into a dense fluid state called a complex coacervate [10, 11].

As the foundation for underwater adhesives, such complex coacervates have several unique and ideal properties, which have been exploited by Sandcastle worms and related organisms for a few hundred million years. They are phase separated fluids that do not disperse when delivered underwater, yet readily adhere to and spread on wet biogenic mineral surfaces. Relevant to medical adhesive needs and specifications, their rheological properties allow them to be delivered through fine gauge cannulas. They are also self-organized in water from pre-polymerized components so significant volume changes, in theory, are not expected to occur upon cure, and repaired tissues are not exposed to toxic solvents, reactants, reaction by-products, or heat generated by exothermic *in situ* polymerization during cure. The underwater bond strengths of the adhesive complex coacervates are greater than the reported bond strengths of natural bioadhesives [12, 13].

Here, using a combination of *in vitro* and *in vivo* approaches, we evaluated a synthetic bioadhesive modeled after the natural underwater adhesive created by the sandcastle worm for cytocompatibility *in vitro* and biocompatibility *in vivo* using a rat calvarial model [14] over a 12 week indwelling period.

Methods

Bioadhesive formulation

Adhesive complex coacervates were prepared as previously reported [11]. Briefly, a commercial non-gelling collagen hydrolysate was amine-modified with ethylenediamine dihydrochloride. A 50 mg/ml aqueous solution of the aminated gelatin at pH 7.4 was added while stirring to a 50 mg/ml aqueous solution of polyphosphodopa containing Ca^{2+} (Ca^{2+}/phosphate sidechain = 0.2) at pH 7.4. The mixture was stirred for 30 minutes and the coacervate phase was collected by centrifugation. Sodium periodate was added to the gelatin complex coacervate at 1:2 ratio to dopa sidechains to initiate crosslinking of the adhesive complex coacervate.

Cell Culture

Direct and indirect contact cell-culture assays were used to evaluate cytocompatibility of the adhesive complex coacervates using a mouse osteoblast (MC3T3-E1) cell line (ATCC, Manassas VA). Briefly, 1 μl of the adhesive was applied into empty wells of 12-well tissue culture plate, and flattened using a Teflon sheet (width 6 mm). 1 ml of α-minimum essential medium (α-MEM) with oxidant $NaIO_4$ at molar ratio of 1:2 to Dopa side chains in the adhesive was added to initiate oxidization. Osteoblasts were plated on top of the bioadhesive at a density of 200,000 cells/well in the α-MEM containing 10% fetal bovine serum, 50 μg/ml penicillin and 50 μg/ml ascorbic acid at 37°C for 48 hours. The osteoblasts were then stained to determine cell viability by live/dead staining (Invitrogen L3224, Carlsbad CA) and imaged with a Nikon Eclipse TE300 inverted scope at 10X. Following imaging, the cells were fixed by immersion in 4% paraformaldehyde in phosphate buffered saline (PBS), pH 7.4 for one hour and then stored in PBS with 0.01% NaN_3. Cell morphology was assessed with immunoflourescent histochemistry using FITC labeled phalloidin (Invitrogen F432, Carlsbad CA), to image actin microfilaments and DAPI to label cell nuclei. Cytocompatibility was evaluated by the presence of viable cells with spread morphology in contact with the surface of the bioadhesive. Cell cultures without the addition of bioadhesive served as controls

Surgical Procedures

All animal procedures were conducted in accordance with the University of Utah Institutional Animal Care and Use Committee (IACUC). Adult male Sprague Dawley rats (200-225 g) were anesthetized via an intraperitoneal injection of ketamine (65 mg/kg), xylazine (7.5 mg/kg), and acepromazine (0.5 mg/kg). After reaching a full level of anesthesia as assessed using tail pinch, animals' heads were shaved, and disinfected with isopropanol and betadyne, followed by transfer to a stereotaxic frame. A midline incision extending the length of the skull was made, and the skin was retracted and the fascia was reflected laterally with a scalpel blade. The surface of the skull bone was dried with cotton-tipped applicators.

To evaluate biocompatibility of the adhesive complex coacervates and its fixation to normal bone in the absence of bone injury, 1 μl of adhesive was placed directly on the surface of the skull (n = 12) and allowed to oxidize. The scalp incision was then closed with 5/0 silk sutures, and the animals were allowed to recover.

To evaluate the biocompatibility in a fracture model, another group of animals had a 3 mm diameter burr hole positioned 3.2 mm posterior to bregma, and 2 mm lateral to bregma cut using a pneumatically-driven trephine under stereotactic control. The circular piece of bone from the craniotomy was retrieved, irrigated with sterile PBS, replaced in the circular hole and aligned in place with the aid of a stereomicroscope. Approximately 1 μl of adhesive was

pipetted into the circular gap (n = 8), while others that served as controls had no adhesive to fix and maintain alignment of the circular piece of bone (n = 4; see Figure 4). In both cases, the scalp incision was closed with 5/0 silk sutures, and the animals were allowed to recover and freely move about until sacrifice.

Euthanasia and tissue preparation

For the surface study in the absence of bone fracture, animals were sacrificed at 2 weeks (n = 6) and at 4 weeks (n = 6). Animals with the cranial fracture were sacrificed at 4 weeks (n = 6) and at 12 weeks (n = 6). All animals were deeply anesthetized via an intraperitoneal injection of ketamine (70 mg/kg) and xylazine (30 mg/kg), and then perfused transcardially with PBS followed by 4% paraformaldehyde, at a flow rate of 50 ml/min. The skulls were dissected with rongers, fine surgical scissors, and microdissection forceps, followed by removal of the brain. Brains and skulls were postfixed separately at 4 °C in 4% paraformaldehyde for 24 hours. Prior to tissue sectioning, skulls were decalcified in 10% EDTA for 4 -5 weeks on a plate rotator at 4°C. The skulls were treated overnight in a 30% sucrose solution, infiltrated with tissue freezing medium (Triangle Biomedical Sciences, Durham, N.C.), and cut in the sagittal plane at a thickness of 30 μm with a cryostat (Leica Microsystems, CM 1950, Wetzlar, Germany). Brains were also postfixed separately at 4°C with 4% paraformaldehyde in PBS overnight. Following postfixation, brains were serially sectioned in the coronal plane at a thickness of 40 μm on a vibratome and examined for signs of damage associated with the use of the bioadhesive.

Histological Staining

GIEMSA working solution (LabChem Inc., Pittsburgh, PA) was prepared by mixing 10 drops of GIEMSA stock solution in 10 ml of DI water. Skull sections were rinsed in PBS, followed by application of GIEMSA working solutions for 12 hours on a plate rotator at 4°C. Next, the section s were rinsed in deionized water, and differentiated in 0.5% acetic acid for approximately 30 seconds. Sections were then washed in deionized water, mounted on microscope slides, covered with Fluormount-G (Southern Biotech, Birmingham AL), and coverslipped.

Immunohistochemistry

All antibodies were diluted in a blocking solution consisting of 4% (v/v) goat serum (Invitrogen, Carlsbad CA), 0.5% (v/v) Triton-X 100, and 0.1% (w/v) sodium azide. Primary antibodies included the pan-macrophage marker CD68 (0.5 μg/ml, AbD Serotec, Raleigh, NC), GFAP (2.4 μg/ml, DAKO, Carpinteria CA), which reacts with an intermediate filament specific to astrocytes, NeuN (2.0 μg/ml, Millipore, Billerica, MA), which binds to elements in neuronal nuclei, and rat IgG (2.0 μg/ml, Southern Biotech, Birmingham, AL) was used to assess the integrity of the blood-brain-barrier (BBB). Tissue sections were batch incubated for 1 hour in a blocking solution at room temperature, followed by incubation with primary antibodies for 12 hours at 4°C. After 3 rinses in PBS at room temperature to remove excess antibody (1 hour/each rinse), appropriate fluorescently-labeled secondary antibodies were applied in block for 1 hour at room temperature, followed by 3 washes in PBS (1 hour/each rinse). All sections were also counterstained with 10 μM DAPI for cell nuclei, mounted on microscope slides, covered with Fluormount-G (Southern Biotech, Birmingham AL), and coverslipped.

Microscopy and imaging

All images were captured with a Coolsnap digital camera (Roper Scientific, Trenton NJ) and a Nikon Eclipse E600 microscope, using identical exposure times and conditions which were optimized for each immunomarker. Additional sections were imaged using an

Olympus FV 1000 confocal microscope. Image light field correction and background subtraction using primary controls were also performed prior to image analysis. Skull sections were imaged at 20X magnification using a computer-controlled x-y stage (Prior, Rockland, MA) which takes a montage of images with ~10% overlap from the previous image. Following imaging, high quality montages of the entire skull section were stitched together using the photomontage function in Adobe Photoshop.

Results

Adhesive complex coacervate behavior in vitro and in vivo

Direct-contact cell-culture assays were used to evaluate cytocompatibility of the gelatin/phosphodopamine copolymer complex coacervate *in vitro*. After 48 hrs of exposure and direct contact with the adhesive, the viability of MC3T3-E1 osteoblast cells (Calcein AM/Ethidium) was 97.2% (Figure 1A). The adhesive, which emits a red autofluorescence, was easy to identify.

Immunoflourescent histochemical analysis showed that the MC3T3-E1 cells attached to, spread on and displayed migratory phenotypes on the surface of the adhesive (Figure 1B). Cells displayed well developed actin stress fibers both on the adhesive surface and along its margins suggesting that direct contact or adjacent exposure produced microenvironmental conditions that where non-toxic and would favor osteoconductive cell behavior.

Cranial Surface Interaction Model

In order to assess biocompatibility *in vivo*, a 1 μl drop of the adhesive mixture was pipetted directly onto the intact skull of adult rats (Figure 2), and assessed 2 and 4 weeks after application using immunohistochemical analysis. When the complex coacervate came in contact with blood, it did not mix (Figure 2B). The blood floated on and over the surface (Figure 2C), but did not penetrate between the adhesive complex coacervate and the underlying normal bone. The interaction with blood appeared to not dilute or otherwise disturb the covalent curing process, which was signaled by a color change from clear to brown (Figure 2) to black (Figure 3). During the indwelling period the animals were freely moving and were permitted unrestrained behavior in their home cages.

Two weeks after application, the adhesive was black and found fixed to the surface of the skull in the same location that it was originally applied where it remained largely intact with little change in volume (Figure 3A). This is in contrast to our experience with two part silicone adhesive that does not stay firmly attached to the surface of the skull, which we have used to anchor silicon microelectrode arrays into circular craniotomies as described in this study [15, 16]. Microscopic examination of tissue sections through the adhesive and underlying demineralized bone showed CD68 immunoreactivity associated with adhesive fragments indicating that it had begun to degrade at the two week time point. Fragmentation was more evident 4 weeks after application with what appeared to be, relatively speaking, a smaller amount of material in the original location of application (Figure 3B). In no case did we observe signs of rejection, necrosis, infection or changes in the underlying skull bone.

Cranial fracture model

The ability of the adhesive to maintain the alignment and fixation of a circular bone piece, as well as to be replaced by new bone was assessed 4 and 12 weeks after reconstruction (Figures 5 – 6). The data was compared to a cohort that received the same treatment but without the adhesive to maintain bone fixation and alignment during the indwelling period. In both groups, animals were allowed to freely move under unrestrained conditions after recovery from anesthesia. Animal weight gain over the indwelling period was the same as

age matched controls (data not shown). Similar to what was reported in the previous animal experiment, the histological data indicated that adhesive degradation was more complete at the longer timepoint and was accompanied by less CD68 immunoreactivity. Fragments of adhesive remained at the 12 week time point indicating that more time was needed for complete resorption to occur.

Uninjured, control sections were associated with some CD68 immunoreactivity that was always observed within bone lacunae (Figure 5A). In the adhesive treatment groups, some adhesive fragments were observed within the defect and on the skull surface near the defect at each timepoint, which was also associated with CD68 immunoreactivity (Figure 5C, E). Adhesive complex coacervate treatment was sufficient to maintain fixation and alignment of the circular piece of bone throughout the 12 week indwelling period. Complete integration of new bone across the defect was not observed in either group 4 weeks after reconstruction (Figures 5C, 6C) and appeared more complete after 12 weeks (Figures 5E, 6E). At 12 weeks, small fragments of adhesive remained near the defect zone. Generally, in both treatment groups there was more new bone formation on the inner surface of the skull than on the outer surface. Microscopic examination showed that newly formed bone became lamellar across the defect suggesting that the adhesive held the bones in place, gradually resorbed and was replaced by new bone without change in alignment.

In contrast, in the control group that did not receive adhesive treatment, we observed in two animals that new bone formation across the defect was incomplete (Figure 5B, 6B) and misaligned (Figure 7). The defect on the skulls of these animals was associated with more fibrous connective tissue, which was not observed in the animals that received the adhesive.

Confocal microscopy was used to analyze the cellular response in more detail. As is shown in Figure 8, highly branched actin staining was observed in osteocytes in uninjured and untreated sections of control skull. A similar phenotype was observed adjacent to the adhesive treated in skull sections, which was consistent with the results of *in vitro* cytocompatiblity studies. In addition, no overt changes to cellular architecture were observed in the underlying brain tissue from the animals in the either study (data not shown).

Discussion

In order to function in skeletal repair applications, fixation technology must address issues of biocompatibility, bone healing, and mechanical integrity [17]. Here, we show that synthetic adhesive complex coacervates, modeled after a natural underwater adhesive used by the marine organism *P. californica* to create protective dwellings in the rough conditions of the intertidal zone, can hold mammalian bone together under wet conditions in vitro and in vivo. In vitro cell contact and indirect exposure assays showed that the adhesive complex coacervate is noncytotoxic, permits cell attachment, spreading, and other phenotypes that suggest that the microenvironment at the surface of the adhesive favors osteoconduction. Moreover, the results of our animal studies indicate that the adhesive attaches to normal bone, can hold broken bones in a particular three-dimensional alignment without being shielded from normal, freely moving behaviors, is biodegradable, does not interfere with normal bone healing, and is eventually replaced by new bone that integrates across the defect while maintaining alignment with the normal adjacent bone.

Available evidence suggests that in the case of bone repair fixation technology an ideal property is the ability of the technology to disappear when it is no longer needed to allow normal loading of the newly integrated bone, as well as to avoid the sequela associated with the FBR, which can include scarring, persistent inflammation, infection, and site specific

osteolysis [18, 19]. In that sense, the bioadhesive described here has an advantage over traditional materials used in bone applications including metal plates [20] and some materials made from tricalcium phosphate, which show poor bioabsorption up to 18 months [21, 22]. The adhesive complex coacervates described here were able to maintain bone fixation in a wet environment, which is similar to the marine environment.

An important observation was the behavior of the adhesive when it came in contact with blood that was oozing from a cranial suture. At the point of contact the blood flowed up, over and around the complex coacervate that was placed on the skull surface. It did not spread between the complex coacervate and the bone interface, or appear to dilute the complex coacervate, thus illustrating its usefulness in surgical fields where active bleeding is common place.

We found that the adhesive was deliverable through a pipette to fill a small gap that contained blood and was able to fix, as well as maintain the alignment of a three millimeter circular piece of bone on the top of the rat skull over a 12 week indwelling period where the animals were allowed free movement immediately after surgery. This was not the case with the cohort where the adhesive was not applied to the gap in which case we observed misalignment, incomplete fusion and excessive fibrous tissue formed at the site of the defect. To spread into the gap and achieve interfacial contact with each side of the defect the bioadhesive had to displace blood after its application and then cure.

The results indicate that the mimetic adhesive was non-cytotoxic and was able to function with an appropriate FBR. We show numerous examples of living cells in contact with the adhesive in vitro surrounded with a limited volume of fluid. In this case, cells appeared as they would under normal tissue culture conditions displaying well defined cytoskeletal features and normal migratory phenotypes suggesting that the materials would be osteoconductive. *In vivo* osteocytes in adjacent bone appeared normal [23]. We found no evidence of necrosis in the bone of adjacent soft tissues above or below the defect site. We found no evidence of infection or indirect inflammation in the underlying or adjacent tissues including the underlying dura or in the brain below, which included an examination of neuronal loss, astrocytosis, and disruption of the blood-brain barrier, which appeared normal (data not shown).

Another important finding, that was alluded to earlier, was that in two of the animals where we did not apply the adhesive to hold the circular piece of bone in place after reconstructive alignment we observed misalignment of the bone and incomplete bone fusion in some places around the bone piece, where the defect contained fibrous connective tissue. This condition was not observed in the cohort that received the adhesive to maintain fixation and alignment. This is in keeping with other observations of critical size calvarial defects associated with fibrous connective tissue [14], however in this case the defect would not have been considered a critical sized defect. Causes of nonunion have been postulated to include instability of the fracture segment, infection, poor blood supply, and soft tissue interposition [24]. In the absence of the adhesive, it is likely that more movement of the bone fragment occurred possibly through grooming or other behaviors as the animals were allowed to move freely immediately after they recovered from the anesthesia following reconstructive surgery.

Many groups have described the FBR in the rat calvarial defect model. Develioğlu et. al showed that foreign body giant cells and activated macrophages accompany normal healing up to 6 months following cranial trephination [25]. Similarly, using the pan-macrophage marker CD68, we observed macrophages within and adjacent to the adhesive during each timepoint of our studies, which is likely part of the normal healing process, and helped

facilitate the breakdown of the adhesive. Moreover, the inflammatory reaction during bone healing has been shown to promote osteoblast differentiation into mature osteocytes [26, 27], thus likely aiding new bone formation following injury. Although we didn't observe complete osteointegration at 12 weeks, sufficient new bone formation did occur to maintain the alignment of the bone across the defect. We suspect that bone remodeling would continue for several months [25, 28]. While some residual adhesive remained 12 weeks after application, we did observe a reduction in the volume of materials and in the overall level of inflammation. Clearly more time will be needed to assess the ultimate fate of the FBR after the adhesive is completely absorbed. Our results are consistent with the degradation kinetics of other degradable materials in the *in vivo* environment [29].

Conclusion

We found that adhesive complex coacervates modeled after a natural adhesive secreted by the Sandcastle worm was capable of holding wet bone together both *in vitro* and *in vivo*. In addition, the adhesive was non-cytotoxic and supported the attachment, spreading, and migration of a commonly used osteoblastic cell line over the course of several days. In animal studies we found that the adhesive was capable of holding its position on normal bone for up to 4 weeks. We also found that the adhesive was capable of maintaining three-dimensional bone alignment in cranial fracture model in freely moving animals over a 12 week indwelling period. Histological evidence indicated that the adhesive was gradually resorbed and replaced by new bone that became lamellar across the defect without loss of alignment, changes in volume or changes in the adjacent uninjured bone. We found no evidence of necrosis, infections, or inflammatory changes in the adjacent soft tissues. The presence of inflammatory cells at the surface of the adhesive was consistent with what has been reported with other fixation methods including metal plates, screws, tacks and cyanoacrylates. Collectively, the results suggest that the adhesive complex coacervates are non-cytotoxic, degradable, osteoconductive and appear suitable for use in the reconstruction of craniofacial fractures.

Acknowledgments

This work was supported by the National Institutes of Health R01EB006463.

References

1. Fritz MA, Koltai PJ. Sequencing and organization of the repair of panfacial fractures. Oper Techn Otolaryng Head Neck. 2002; 13(4):261–4.
2. Gruss JS. Advances in craniofacial fracture repair. Scand J Plast Reconstr Surg Hand Surg Suppl. 1995; 27:67–81. [PubMed: 7795294]
3. Gruss JS, Mackinnon SE, Kassel EE, Cooper PW. The role of primary bone grafting in complex craniomaxillofacial trauma. Plast Reconstr Surg. 1985; 75(1):17–24. [PubMed: 3880900]
4. Kelly KJ, Manson PN, Vander Kolk CA, Markowitz BL, Dunham CM, Rumley TO, et al. Sequencing LeFort fracture treatment (Organization of treatment for a panfacial fracture). J Craniofac Surg. 1990; 1(4):168–78. [PubMed: 2098175]
5. Manson PN, Crawley WA, Yaremchuk MJ, Rochman GM, Hoopes JE, French JH Jr. Midface fractures: advantages of immediate extended open reduction and bone grafting. Plast Reconstr Surg. 1985; 76(1):1–12. [PubMed: 3892561]
6. Gosain AK, Song L, Corrao MA, Pintar FA. Biomechanical evaluation of titanium, biodegradable plate and screw, and cyanoacrylate glue fixation systems in craniofacial surgery. Plast Reconstr Surg. 1998; 101(3):582–91. [PubMed: 9500375]
7. Jensen RA, Morse DE. The bioadhesive of Phragmatopoma californica tubes: a silk-like cement containing L-DOPA. J Comp Physiol B. 1988; 158(3):317–24.

8. Stewart RJ, Weaver JC, Morse DE, Waite JH. The tube cement of Phragmatopoma californica: a solid foam. J Exp Biol. 2004; 207(Pt 26):4727–34. [PubMed: 15579565]
9. Zhao H, Sun C, Stewart RJ, Waite JH. Cement proteins of the tube-building polychaete Phragmatopoma californica. J Biol Chem. 2005; 280(52):42938–44. [PubMed: 16227622]
10. Shao H, Bachus KN, Stewart RJ. A water-borne adhesive modeled after the sandcastle glue of P. californica. Macromol Biosci. 2009; 9(5):464–71. [PubMed: 19040222]
11. Shao H, Stewart RJ. Biomimetic underwater adhesives with environmentally triggered setting mechanisms. Adv Mater. 2010; 22(6):729–33. [PubMed: 20217779]
12. Burkett JR, Wojtas JL, Cloud JL, Wilker JJ. Method for measuring the adhesion strength of marine mussels. J Adhesion. 2009; 85(9)
13. Sun C, Fantner GE, Adams J, Hansma PK, Waite JH. The role of calcium and magnesium in the concrete tubes of the sandcastle worm. J Exp Biol. 2007; 210(Pt 8):1481–8. [PubMed: 17401131]
14. Frame JW. A convenient animal model for testing bone substitute materials. J Oral Surg. 1980; 38(3):176–80. [PubMed: 6928181]
15. Biran R, Martin DC, Tresco PA. Neuronal cell loss accompanies the brain tissue response to chronically implanted silicon microelectrode arrays. Exp Neurol. 2005; 195(1):115–26. [PubMed: 16045910]
16. Biran R, Martin DC, Tresco PA. The brain tissue response to implanted silicon microelectrode arrays is increased when the device is tethered to the skull. J Biomed Mater Res A. 2007; 82(1): 169–78. [PubMed: 17266019]
17. Oreffo RO, Triffitt JT. In vitro and in vivo methods to determine the interactions of osteogenic cells with biomaterials. J Mater Sci Mater Med. 1999; 10(10/11):607–11. [PubMed: 15347974]
18. Cunningham LL. The use of calcium phosphate cements in the maxilofacial region. J Long-Term Eff Med. 2005; 15(6):609–16.
19. Fleckenstein KB, Cuenin MF, Peacock ME, Billman MA, Swiec GD, Buxton TB, et al. Effect of a hydroxyapatite tricalcium phosphate alloplast on osseous repair in the rat calvarium. J Periodontol. 2006; 77(1):39–45. [PubMed: 16579701]
20. Haug RH, Cunningham LL, Brandt M. Todd. Plates, screws, children: their relationship in craniomaxillofacial trauma. J Long-Term Eff Med. 2003; 13(4):271–87.
21. Froum S, Stahl SS. Human intraosseous healing responses to the placement of tricalcium phosphate ceramic implants. II. 13 to 18 months. J Periodontol. 1987; 58(2):103–9. [PubMed: 3469399]
22. Handschel J, Wiesmann HP, Stratmann U, Kleinheinz J, Meyer U, Joos U. TCP is hardly resorbed and not osteoconductive in a non-loading calvarial model. Biomaterials. 2002; 23(7):1689–95. [PubMed: 11922472]
23. Tanaka-Kamioka K, Kamioka H, Ris H, Lim SS. Osteocyte shape is dependent on actin filaments and osteocyte processes are unique actin-rich projections. J Bone Miner Res. 1998; 13(10):1555–68. [PubMed: 9783544]
24. Schmitz JP, Schwartz Z, Hollinger JO, Boyan BD. Characterization of rat calvarial nonunion defects. Acta Anat (Basel). 1990; 138(3):185–92. [PubMed: 2389661]
25. Develioglu H, Saraydin SU, Bolayir G, Dupoirieux L. Assessment of the effect of a biphasic ceramic on bone response in a rat calvarial defect model. J Biomed Mater Res A. 2006; 77(3):627–31. [PubMed: 16514598]
26. Gortz B, Hayer S, Redlich K, Zwerina J, Tohidast-Akrad M, Tuerk B, et al. Arthritis induces lymphocytic bone marrow inflammation and endosteal bone formation. J Bone Miner Res. 2004; 19(6):990–8. [PubMed: 15125796]
27. Rifas L, Arackal S, Weitzmann MN. Inflammatory T cells rapidly induce differentiation of human bone marrow stromal cells into mature osteoblasts. J Cell Biochem. 2003; 88(4):650–9. [PubMed: 12577299]
28. Honma T, Itagaki T, Nakamura M, Kamakura S, Takahashi I, Echigo S, et al. Bone formation in rat calvaria ceases within a limited period regardless of completion of defect repair. Oral Dis. 2008; 14(5):457–64. [PubMed: 18938272]

29. Stephan SJ, Tholpady SS, Gross B, Petrie-Aronin CE, Botchway EA, Nair LS, et al. Injectable tissue-engineered bone repair of a rat calvarial defect. Laryngoscope. 2010; 120(5):895–901. [PubMed: 20422682]

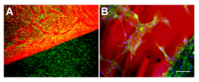

Figure 1. In vitro cytocompatibility

After 48 hrs exposure to the adhesive complex coacervate, osteoblast viability (live/dead) and cell morphology (phalloidin-FITC staining) assays showed cell contact spreading and proliferation. A) Adhesive associated with osteoblast attachment on tissue culture polystyrene, showing homogeneous staining both on the polystyrene and the adhesive. B) Magnified view from A, showing osteoblast attachment directly to the adhesive. Adhesive (red), actin (green), and DAPI (blue). Scalebar = 100 μm.

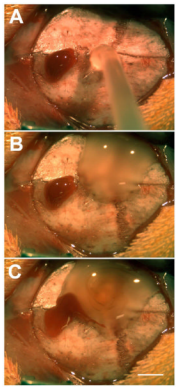

Figure 2. Blood-complex coacervate interaction

During implantation, a drop of blood (A) was allowed to come into contact with the adhesive complex coacervate (B, C). The blood did not mix with the complex coacervate, but was observed to float over the surface, and did not disturb the curing process. Scalebar = 2 mm.

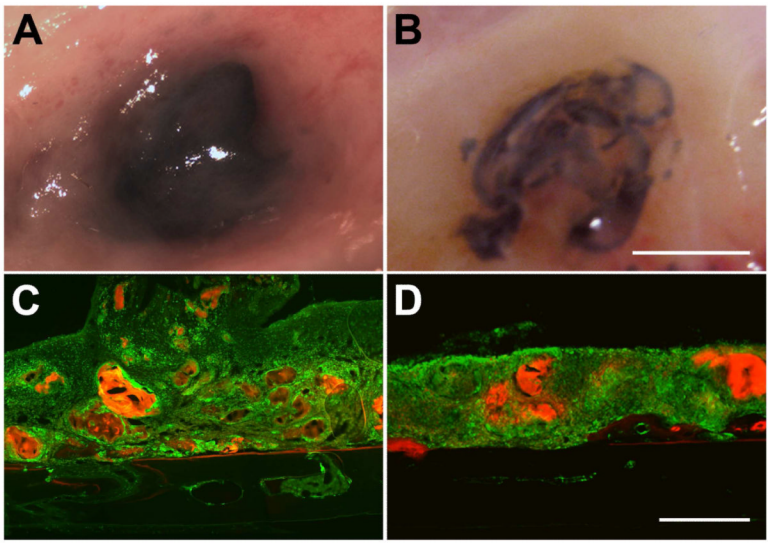

Figure 3. Analysis of the adhesive on skull surface

2 weeks (A,C) following the application of 1 μl of adhesive directly on the surface of the skull, the adhesive was found to be largely intact. Skull sections showed CD68 immunoreactivity (green) associated with adhesive fragments (red). Adhesive degradation was more obvious at 4 weeks (B,D). A and B show representative views of the adhesive and associated tissue at the time of sacrifice. C and D show representative sagittal skull sections through the center of the adhesive droplet. Sections are oriented with the side in contact with the dura down and the nose of the animal to the left. Scalebar in B, same as A, and = 5 mm. Scalebar in D, same as C, and = 500 μm.

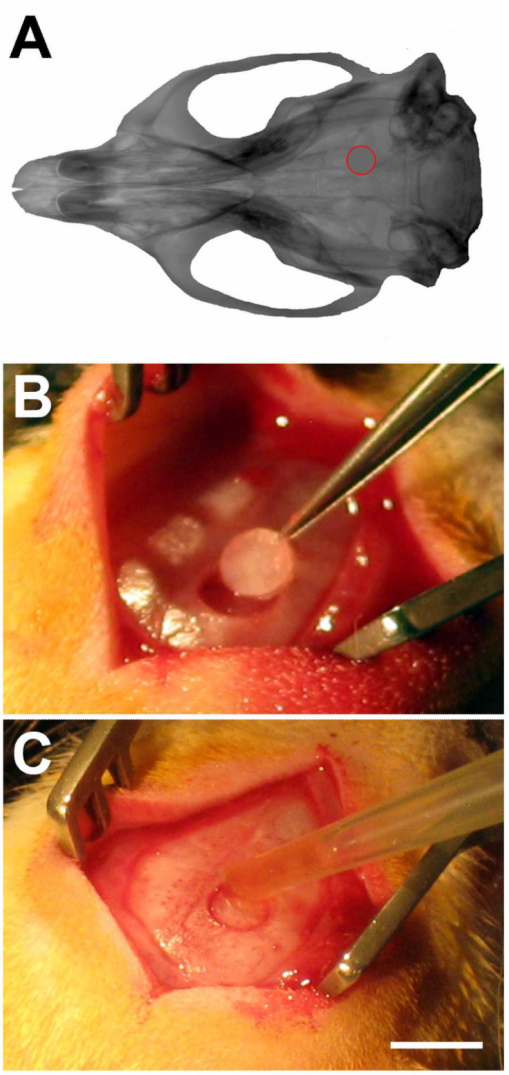

Figure 4. Rat calvarial model

A) CT reconstruction of rat skull, with location of the craniotomy shown in red. B) Rats had a 3 mm diameter burr hole with the center positioned −3.2 mm from bregma, and 2 mm lateral to bregma cut via trephination. C) The craniotomy was replaced with 1 μl of adhesive (n = 8). Additional sham animals had the craniotomy replaced without adhesive (n = 4). Scalebar in C, same as B, and = 5 mm.

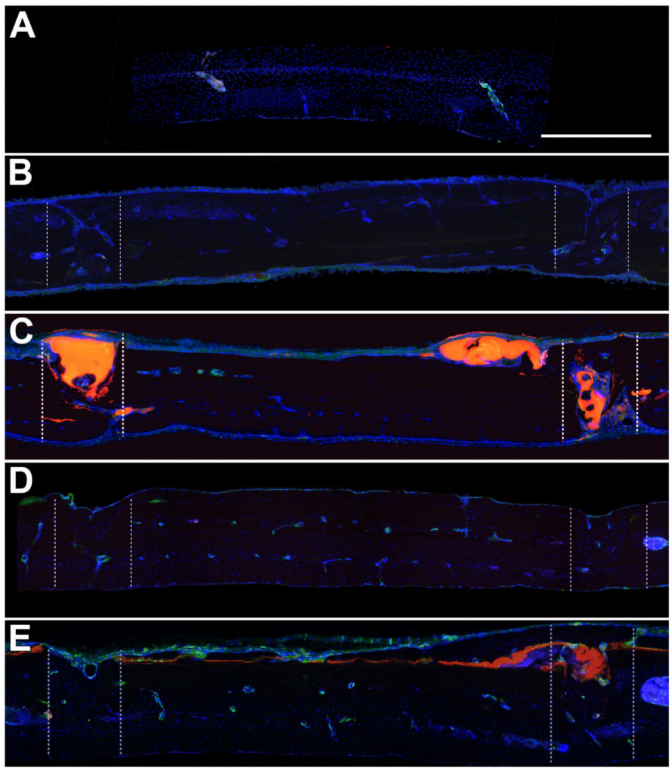

Figure 5. CD68 Immunoreactivity

A) Representative sagittal control skull section showing minimal CD68 immunoreactivity, which was usually associated with marrow cavities. B) Representative sagittal section from the sham group at 4 weeks, showing fusion of the bones on one side and incomplete fusion on the other. C) Representative sagittal skull section at 4 weeks from the adhesive group showing adhesive within and on the surface of the craniotomy, associated with CD68 immunoreactivity. The adhesive was sufficient to maintain the placement of the craniotomy. Complete bone fusion was not observed on either side of the craniotomy. D) Representative sagittal section from the sham group at 12 weeks, showing fusion of the craniotomy on both sides. E) Representative sagittal skull section at 12 weeks from the adhesive group showing adhesive within and on the surface of the craniotomy, associated with CD68 immunoreactivity. Bone fusion was achieved by 12 weeks. Sections are oriented with the side in contact with the dura down and the nose of the animal to the left. CD68 (green), DAPI (blue), bioadhesive (red). Zones of the craniotomy are shown in dashed lines. Scalebar = 500 μm.

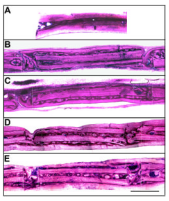

Figure 6. GIEMSA histology

A) Representative sagittal control skull section showing GIEMSA staining in normal uninjured rat calvaria. B) Representative sagittal section from the sham group at 4 weeks, showing fusion of the bones on one side and incomplete fusion on the other. C) Representative sagittal skull section at 4 weeks from the adhesive group showing adhesive within and on the surface of the craniotomy. The adhesive was sufficient to maintain the placement of the craniotomy. Complete bone fusion was not observed on either side of the craniotomy. D) Representative sagittal section from the sham group at 12 weeks, showing fusion of the craniotomy on both sides. E) Representative sagittal skull section at 12 weeks from the adhesive group showing adhesive within and on the surface of the craniotomy. Bone fusion was achieved by 12 weeks. Sections are oriented with the side in contact with the dura down and the nose of the animal to the left. Adhesive appears black with GIEMSA staining. Zones of the craniotomy are shown in dashed lines. Scalebar = 500 μm.

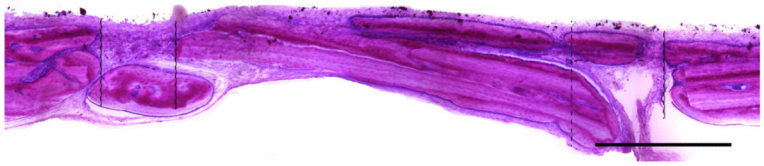

Figure 7. Unfused shams

At both 4 and 12 weeks, 1 out of 2 sham animals showed post-surgical movement of the craniotomy, which caused the craniotomies to not fuse. This phenotype was not observed in any of the animals implanted with the adhesive. Zones of the craniotomy are shown in dashed lines. Sections are oriented with the side in contact with the dura down and the nose of the animal to the left. Scalebar = 500 μm.

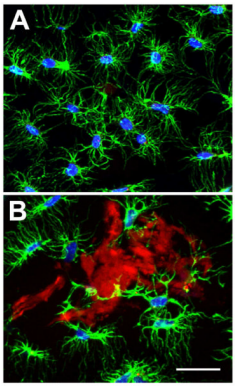

Figure 8. Cellular association with adhesive complex coacervates *in vivo*

A) Representative confocal image showing actin (green) and DAPI (blue) staining of osteocytes in normal uninjured rat calvaria. B) Representative confocal imaging showing osteocyte association with adhesive fragments (red) within the craniotomy region at 12 weeks. Scalebar = 50 μm.